Measurement of the 2s 2p2(4P) 3s 3P2 lifetime in N II by beam-foil-laser spectroscopy

T. Bastin, Y. Baudinet-Robinet, P.-D. Dumont, H.-P. Garnir

Classification
Physics Abstracts
32.70F — 32.70C — 32.90

Measurement of the 2s $2p^2(^4P)$ 3s $^3P_2$ lifetime in N II by beam-foil-laser spectroscopy

T. Bastin (*), Y. Baudinet-Robinet (**), P.-D. Dumont and H.-P. Garnir

Institut de Physique Nucléaire Expérimentale, Université de Liège, Sart Tilman B 15, B-4000 Liège, Belgium

(*Received 17 May 1993, accepted in final form 5 July 1993*)

Résumé. — Nous avons mesuré avec précision la durée de vie radiative du niveau 2s $2p^2(^4P)$ 3s $^3P_2$ de N II par la méthode de spectroscopie faisceau-lame-laser. La durée de vie obtenue ($\tau = 0.456 \pm 0.020$ ns) est plus courte que celles mesurées précédemment, par spectroscopie faisceau-lame, pour le terme 3s' ^3P de N II. Aucune valeur théorique de la durée de vie de ce terme n'est actuellement disponible.

Abstract. — An accurate value for the radiative lifetime of the 2s $2p^2(^4P)$ 3s $^3P_2$ level in N II has been obtained using the beam-foil-laser spectroscopy method. The result ($\tau = 0.456 \pm 0.020$ ns) is shorter than the beam-foil lifetime values reported previously for the 3s' ^3P term. No theoretical value for the lifetime of this term is available at the present time.

1. Introduction.

In the beam-foil-laser spectroscopy method, described in detail in [1-3], a fast ion beam crosses at right angles successively a carbon foil and the intracavity beam of a tunable cw dye laser. The first excitation of the ions in the foil is nonselective whereas the second excitation in the laser field is selective. In this method, cascade-free decay curves reducing to single exponentials are recorded and accurate lifetimes are deduced from the analyses of these curves. The lifetime of the 3s' $^3P(1s^2\ 2s\ 2p^2(^4P)\ 3s\ ^3P)$ term in N II has been measured previously [4-6] by the beam-foil spectroscopy method in which the ion excitation is nonselective. Thus, the lifetime is deduced from the analyses of decay curves corresponding to a sum of exponentials which limits the accuracy of this method. In the present work, an accurate lifetime value for the 3s' $^3P_2$ level in N II has been obtained by the beam-foil-laser spectroscopy method. To our knowledge, no theoretical lifetime has been reported for this term.

(*) Research Assistant of the Belgian FNRS.
(**) Senior Research Associate of the Belgian FNRS.

2. Experiment.

The detailed description of the experimental arrangement has been given in [1, 2]. In the present experiment, the wavelength of the dye laser is tuned to resonance with the $4s\ ^3P_2^0 - 3s'\ ^3P_2$ transition in N II at 661.362 nm and the $2p^3\ ^3D_3^0 - 3s'\ ^3P_2$ transition at

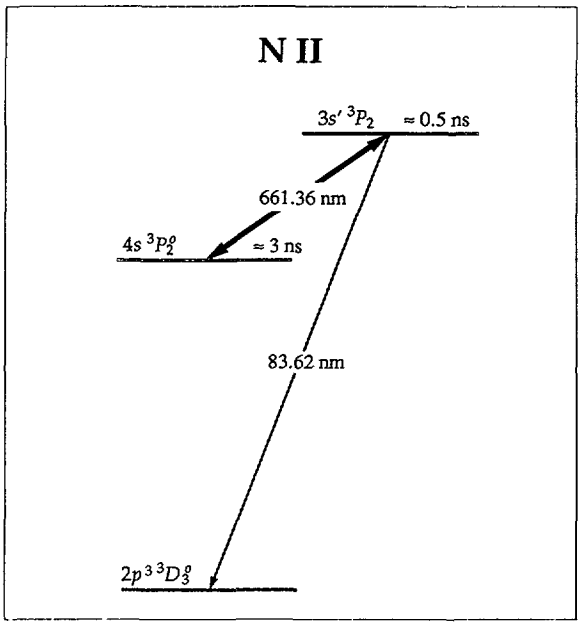

Fig. 1. — Laser induced transition and observed line for the lifetime measurement of the $3s'\ ^3P_2$ level in N II.

Table I. — *Summary of experimental conditions for the lifetime measurement of the* N II $3s'\ ^3P_2$ *level.*

N_2^+ beam energy (MeV) before the foil	1.050 ± 0.005
Ion velocity after the foil (mm/ns)	2.46 ± 0.05
Ion beam cross section (mm^2)	0.6 x 6.0
Dye	DCM
Power of the argon laser pump (W)	22
Dye intracavity power (W)	≈25
Dye laser beam diameter (mm)	≈1
Carbon foil thickness ($\mu g/cm^2$)	20 ± 2 and 15 ± 2
Carbon foil size (mm^2)	1.5 x 7.0
Distance between foil and laser beam axis (mm)	≈3
Ion beam portion viewed by the spectrometer (mm)	≈0.6

83.619 nm is observed with a Seya-Namioka type spectrometer equipped with channeltron detectors (see Fig. 1). The experimental conditions are summarized in table I.

The intensities of the 83.619 nm line when the laser is switched on and off are monitored as a function of the distance traveled by the ions downstream from the interaction region. The curve obtained by the difference of these intensities (called a BFL decay curve) is a single exponential. The lifetime of the upper level of the laser induced transition is much shorter than that of the lower level of this transition (see Fig. 1 where approximate values of the level lifetimes are quoted). Thus, during the 3 mm distance between the foil and the laser field (see Tab. I), the population of the studied upper level has strongly decreased whereas that of the lower level is practically unchanged. Under these conditions, observable repopulation of the studied level is expected to occur in the laser field.

During the measurements, the wavelength of the dye laser is automatically controlled and corrected, if necessary. The intracavity power of the dye laser is recorded during each photon measurement so that the photon differences (laser on and laser off) can be normalized to take into account small variations of this power. The ion velocity before the foil is deduced from the accurate measurement of the Van de Graaff accelerator voltage. The slowing down of the ions in the foil is calculated using an empirical relation that fits tabulated energy loss data [7]. The whole experiment is controlled by a network of small computers and the data are collected and analysed on line [8].

3. Results and discussion.

At the exit of the laser interaction region, the difference of the laser-on and laser-off intensities for the 83.619 nm line amounts to about 5 % of the laser-off intensity. To obtain a statistically significant BFL decay curve, it is necessary to accumulate several BFL decay curves, each recorded in a reasonable time for maintaining stable experimental conditions. In order to cancel small systematic errors, decay data were recorded by moving the foil-laser interaction region successively parallel and antiparallel to the ion beam direction. No significant difference appeared between the two groups of curves obtained in this way.

For each BFL decay curve, twelve data points along a total distance of 2.2 mm were taken. These decay curves were accumulated until the statistical error (one standard deviation) in the difference of photon numbers (with and without laser excitation) at the maximum of the BFL curve was equal to $\approx$ 14 % of this difference. This corresponded to a laser-off photon counts of about 40 000 and a difference of photon numbers of about 2 000. Finally, a sample of 10 accumulated BFL decay curves of similar statistical quality was obtained. Each of these 10 curves were adjusted to a single exponential using a least-squares fitting program [9]. The 10 estimated lifetimes are weighted by taking into account the errors given by the fitting program. The weighted mean value of the 10 estimated lifetimes is

$$\tau = 0.456 \pm 0.018 \text{ ns} \quad (1)$$

where the quoted error represents the standard deviation of the mean value estimated from the dispersion of the weighted sample. We have also summed the 10 BFL decay curves and obtained the total BFL decay curve shown in figure 2. The error bars represent the statistical uncertainties (plus and minus one standard deviation). The standard deviation, at the position x, is $s(x) = (n^L(x) + n^0(x))^{1/2}$ where $n^L(x)$ and $n^0(x)$ are the numbers of photons counted, with and without laser excitation, respectively. The lifetime value obtained from the adjustment of this curve to one exponential ($\chi^2 = 0.6$) is

$$\tau = 0.456 \pm 0.020 \text{ ns} \quad (2)$$

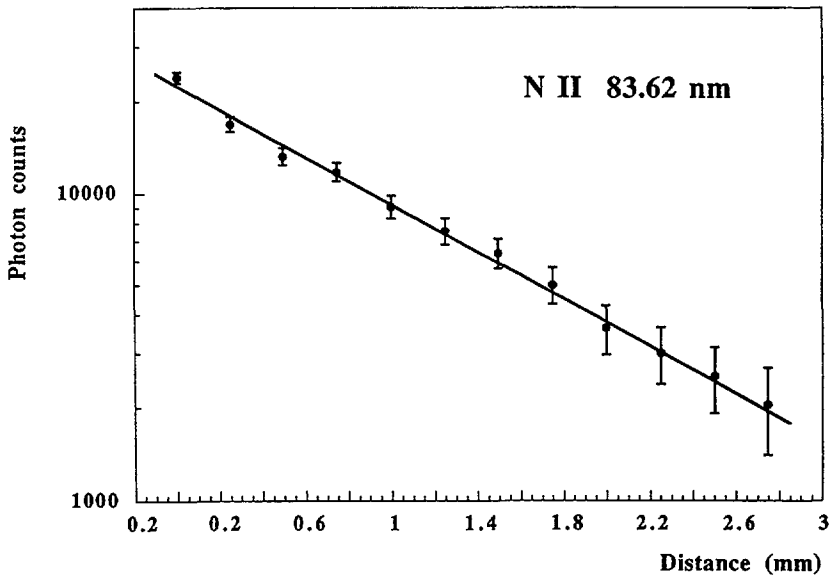

Fig. 2. — Total BFL decay curve recorded for the $2p^3\ ^3D^0_3$-$3s'\ ^3P_2$ transition at 83.619 nm using 1.05 MeV N_2^+ ions. The error bars represent the statistical uncertainty (plus and minus one standard deviation).

where the quoted error represents the standard deviation given by the fitting program. The lifetime values and the errors obtained by the two analysis methods are in very good agreement. The total error in the lifetime value is obtained by combining a 2 % error due to the uncertainty in the ion velocity after the foil with the statistical error given in relation (1). The final lifetime result is presented in table II together with the lifetime values available [4-6]. The previous lifetime values have all been obtained by beam-foil spectroscopy and concern the $3s'\ ^3P$ term because the individual fine-structure components of the $2p^3\ ^3D^0$-$3s'\ ^3P$ transition have not been resolved. The beam-foil decay curves have been decomposed into a sum of at least two exponentials. The three beam-foil results are in agreement, within the quoted error (one standard deviation). The BFL lifetime is more accurate and significantly shorter than the most precise beam-foil lifetime reported by Kernahan *et al.* [6].

Table II. — *Lifetime results for the* $3s'\ ^3P_2$ *level in* N II.

Lifetime (ns)	Method
0.57 ± 0.09	Beam-foil spectroscopy [4]
0.51 ± 0.1	Beam-foil spectroscopy [5]
0.554 ± 0.028	Beam-foil spectroscopy [6]
0.456 ± 0.020	Beam-foil–laser spectroscopy (this work)

References

[1] Dumont P. D., Garnir H. P., Baudinet Y., El Himdy A., *Nucl. Instrum. Methods* **B 35** (1988) 191.
[2] Baudinet Y., Dumont P. D., Garnir H. P., El Himdy A., *Phys. Rev. A* **40** (1989) 6321.
[3] Baudinet Y., Garnir H. P., Dumont P. D., Résimont J., *Phys. Rev. A* **42** (1990) 1080.
[4] Buchet J. P., Poulizac M. C., Carre M., *J. Opt. Soc. Am.* **62** (1972) 623.
[5] Dumont P. D., Biémont E., Grevesse N., *J. Quant. Spectrosc. Radiat. Transfer* **14** (1974) 1127
[6] Kernahan J. A., Livingston A. E., Pinnington E. H., *Can. J. Phys.* **52** (1974) 1895.
[7] Garnir-Monjoie F. S., Garnir H. P., Baudinet-Robinet Y., Dumont P. D., *J. Physique* **41** (1980) 599.
[8] Monjoie F., Garnir H. P., *Comput. Phys. Commun.* **61** (1990) 267.
[9] Monjoie F., Garnir H. P., *Comput. Phys. Commun.* **74** (1993) 1.

Classification
Physics Abstracts
68.10 — 68.15 — 61.30 — 61.25

Static wetting behaviour of diblock copolymers

D. Ausserre, V. A. Raghunathan and M. Maaloum

Equipe de Physique de l'Etat Condensé. C.N.R.S. U.R.A. 807, Université du Maine, B.P. 535, 72017 Le Mans Cedex, France

(*Received 23 February 1993, revised and accepted 16 July 1993*)

Abstract. — Thin liquid films of ordered diblock copolymers deposited on a solid substrate form a multilayer stacking parallel to the solid surface. A multilayer with a finite extend can be stable, metastable, or unstable, depending on the relative values of the surface energies of the various interfaces. The spreading parameter and chemical potential of a n-layer are derived, and used for classifying all possible situations. It is shown that only mono- and bilayers can be stable, and that non-wetting multilayers are subjected to a long-time piling up instability, leading in practice to the formation of characteristic ziggourat-like structures.

A diblock copolymer is made of two polymer chains with different chemical compositions A and B linked together end to end. Depending on the temperature, these materials are found in two different states. For $T > T_{OD}$, A and B are mixed and form a homogeneous melt. On the other hand, for $T < T_{OD}$, A and B species phase-separate and form miccrodomains with one dimension at least comparable to the chain size. T_{OD} is called the microphase separation temperature or the order-disorder transition temperature [1]. In the case of symmetric diblock copolymers, which have almost equal volume fractions of A and B, the microphase structure is lamellar. In thin films of these materials deposited on a solid substrate, these layers orient parallel to the substrate. In the present paper, we examine the wetting properties of these copolymer melts.

The wetting behaviour of a simple liquid A on a solid surface is controled by the spreading parameter [2], defined by

$$S_A = \gamma_{SV} - \gamma_{LS}^A - \gamma_{LV}^A \tag{1}$$

where γ_{SV}, γ_{LS}^A and γ_{LV}^A are the surface tensions associated with the solid-vapour, liquid-solid and liquid-vapour interfaces, respectively. If S_A is positive, the liquid spreads on the solid surface. Otherwise it does not wet the surface and forms a drop with a well-defined contact angle θ_A given by the Young relation

$$\gamma_{LV}^A \cos \theta_A = \gamma_{SV} - \gamma_{LS}^A . \tag{2}$$

Equations (1) and (2) hold good for any homogeneous liquid including polymer melts.

1. Spreading parameter of a monolayer.

Consider a monolayer of a symmetric diblock copolymer lying on a solid substrate, as illustrated in figure 1. The free energy per chain in such a film can be written as [3]

$$F_c = (3/2)\,\alpha k_B T(\ell/R_0)^2 + (Na^3/\ell)(\gamma_{AB} + \gamma^B_{LV} + \gamma^A_{LS}) \tag{3}$$

where ℓ is the monolayer thickness, α a numerical factor of the order of 1, k_B the Boltzmann constant, N the monomer index of the polymer, a the typical monomer size and $R_0 = aN^{(1/2)}$ This phenomenological expression is found to be able to describe most of the observed properties of the lamellar phase of copolymers in the strong segregation limit, i.e. far from the order disorder transition. In the following we assume the above expression to be valid for a wide range of values of ℓ.

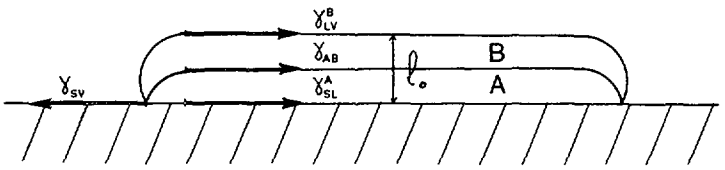

Fig. 1. — Schematic cross-section of a finite monolayer AB on a solid substrate. The equilibrium thickness ℓ_0 is obtained for a balance of the different surface tensions, which can be viewed as forces per unit length of the edge.

The free energy of the system is therefore given by

$$F_1 = mF_c + \gamma_{SV}(A_S - A_P) \tag{4}$$

where A_S is the total surface area of the solid, A_P the area covered by the copolymer and m the total number of polymer chains in the melt. Taking the energy of the bare solid as the reference, one can replace F_1 by

$$\Delta F_1 = F_1 - \gamma_{SV} A_S .$$

Since $A_P = mNa^3/\ell$, one gets

$$\Delta F_1 = m\left((3/2)\,\alpha k_B T(\ell/R_0)^2 - S_1 Na^3/\ell\right) \tag{5}$$

with

$$S_1 = \gamma_{SV} - \gamma^A_{LS} - \gamma^B_{LV} - \gamma_{AB} . \tag{6}$$

When S_1 is negative, ΔF_1 has a minimum at $\ell = \ell_0$, with

$$\frac{\ell_0}{R_0} = \left(-\frac{S_1 aR_0}{3\,\alpha k_B T}\right)^{1/3} \tag{7}$$

and

$$\Delta F_1(\ell_0) = -\,(3/2)\,S_1 A_P .$$

If one includes the possibility of multilayer stacking, the minimum of ΔF_1 does not give necessarily the most stable state. Hence the monolayer at ℓ_0 could be metastable. When $S_1 > 0$, ΔF_1 has no minimum for any $\ell > 0$ within the framework of equation (3), and the melt totally spreads on the solid surface. The final thickness of the film in this case will be determined by the disjoining pressure due to the van der Waals forces. The sign of S_1 therefore determines the wetting behaviour of the monolayer. Note that :

1) The spreading condition $S_1 > 0$ is much more difficult to realize than for a simple liquid, due to the additional surface tension γ_{AB} ;

2) The fact that the two pure species A and B taken separately wet a given solid surface, does not imply that the same is true for the copolymer ;

3) We call A the species in contact with the solid, which implies :

$$\gamma^A_{LS} + \gamma^B_{LV} < \gamma^B_{LS} + \gamma^A_{LV} . \tag{8}$$

2. Energy of a copolymer bilayer.

The structure of the bilayer requires that the same chemical species be in contact with both the solid and the vapour (Fig. 2). We take this to be the species A. In other words, we assume that the inequality,

$$\gamma^A_{LS} + \gamma^A_{LV} < \gamma^B_{LS} + \gamma^B_{LV}$$

is satisfied. In terms of $\Delta\gamma_{LS} = \gamma^B_{LS} - \gamma^A_{LS}$ and $\Delta\gamma = \gamma^B_{LV} - \gamma^A_{LV}$, the above inequality can be written as

$$\Delta\gamma + \Delta\gamma_{LS} > 0 . \tag{9}$$

We will always assume in the following that both (8) and (9) are satisfied, which reads $\Delta\gamma_{LS} > |\Delta\gamma|$. It means that we impose the preference of the solid for A to be stronger than the preference of the free surface for any species. If it was not the case, we should call A the polymer at the free surface and invert LV and LS indexes everywhere ; then we could use directly all the results which follow. Indeed, as we consider geometries where the liquid-solid and liquid-vapor interface have the same area, they play a symmetric role in the expression of the free energy. Hence conditions (8) and (9) do not restrict the generality of the analysis.

Let ℓ_1 and ℓ_2 be the thicknesses of the two layers in the bilayer (Fig. 2). For fixed A_p, one can exchange molecules between the two layers and hence ℓ_1 and ℓ_2 have to be determined by minimizing the energy of the system with respect to one of them. From volume conservation we have

$$A_p = mNa^3/(\ell_1 + \ell_2) .$$

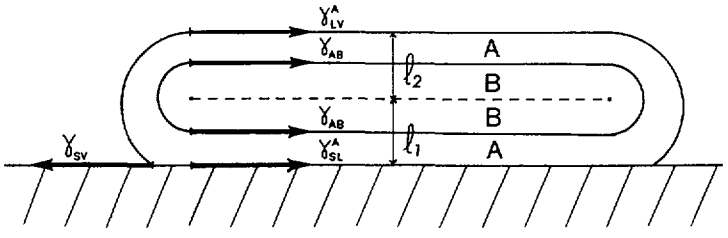

Fig. 2. — Schematic cross-section of a finite bilayer ABBA on a solid. The fictive interface BB is represented by dotted lines.

The total energy of the system is

$$\Delta F_2 = (3/2)\,\alpha k_B T\{m_1 \ell_1^2 + m_2 \ell_2^2\}/R_0^2 + \{2\,\gamma_{AB} + \gamma_{LV}^A + \gamma_{LS}^A - \gamma_{SV}\}\,A_P \qquad (10)$$

with $m_1 = A_P \ell_1/(Na^3)$ and $m_2 = A_P \ell_2/(Na^3)$.

Minimization of ΔF_2 with respect to ℓ_1 at constant A_P leads to $\ell_1 = \ell_2$, i.e., the two layers have the same thickness. The minimum of the energy is given by

$$\Delta F_2 = m\left((3/2)\,\alpha k_B T(\ell/R_0)^2 - S_2 Na^3/\ell\right) \qquad (11)$$

where

$$S_2 = (1/2)\,S_A - \gamma_{AB}\,.$$

Note that this is the same expression as that for ΔF_1, but with S_1 replaced by S_2. When $S_2 < 0$, ΔF_2 has a minimum and the bilayer is at least a metastable state. For $S_2 > 0$, the bilayer is unstable and spreads on the solid surface.

3. Wetting behaviour of a multilayer.

In the following discussion we assume that all the layers in the film have the same area. As we are considering only the stable and metastable states, this does not exclude any equilibrium possibility. For n layers the expression for the free energy generalizes to

$$\Delta F_n = m\left((3/2)\,\alpha k_B T(\ell/R_0)^2 - S_n Na^3/\ell\right)\,. \qquad (12)$$

All the layers in the film have the same thickness ℓ, since they have the same area. The spreading parameter S_n now becomes

$$S_n = (1/n)(S_A - \Delta\gamma^{up}) - \gamma_{AB} \qquad (13)$$

where

$$\Delta\gamma^{up} = \gamma \text{ for } n \text{ odd}$$
$$= 0 \text{ for } n \text{ even}\,.$$

The multilayer is at least metastable if $S_n < 0$. This condition is always satisfied for sufficiently large n, since $S_n \to -\gamma_{AB}$ as $n \to \infty$. The free energy of a metastable n-layer state is

$$\Delta F_n = -(3/2)\,nS_n A_P$$

with $A_P = mNa^3/(n\ell)$. Minimizing equation (12) the equilibrium layer thickness is found to be

$$\frac{\ell_0(n)}{R_0} = \left(-\frac{S_n aR_0}{3\,\alpha k_B T}\right)^{1/3} \qquad (14)$$

Dividing ΔF_n by m gives the chemical potential

$$\mu_n = \left(\frac{3}{2}\right)(3\,\alpha k_B T)^{1/3}\,(aR_0 S_n)^{2/3} \qquad (15)$$

As μ_n is a monotonic function of $|S_n|$, all the stability analysis can be easily carried out in terms of the spreading parameter.

Dividing S_n by γ_{AB}, one gets the dimensionless spreading parameter

$$\sigma_n = (1/n)(\sigma_A - \delta^{up}) - 1 \qquad (16)$$

where

$$\sigma_A = S_A/\gamma_{AB} \quad \text{and} \quad \delta^{up} = \Delta\gamma^{up}/\gamma_{AB} .$$

Note that

$$\begin{aligned} \delta^{up} = \delta &= (\gamma^B_{LV} - \gamma^A_{LV})/\gamma_{AB} \qquad \text{for } n \text{ odd} \\ &= 0 \qquad\qquad\qquad\qquad\quad \text{for } n \text{ even} . \end{aligned}$$

These dimensionless quantities are used in the following discussion. As the behaviour of the system is determined by the sign of $d\sigma_n/dn$ and the sign and magnitude of σ_n, we consider the various possibilities below.

3.1 $\sigma_A - \delta^{up} < 0$. — In this case σ_n is negative for all n all states are metastable. Further, as μ_n decreases with increasing n, a given film would tend to decrease its surface area by increasing the number of layers in it. This results in what may be called a piling up instability. Figure 3 illustrates the situation where condition 3.1 holds for both parities. Note that the continuous lines in the figure are only guides for the eye, since σ_n is defined only for integer values of n. Figure 4 shows an experimentally observed example of such a piled-up ziggourat-like structure obtained after very long time from an initially uniform 3-layers film. Because of its circular symmetry, we call it Babel tower. Each layer in this pyramidal structure has a different area, suggesting that it is a transient state involved in the evolution process.

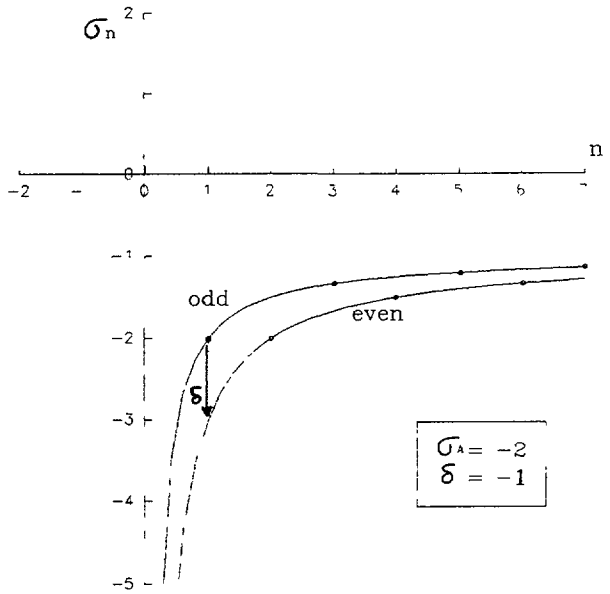

Fig. 3. — Variation of σ_n *versus* n for $\sigma_A = -2$ and $\delta = -1$. σ_n is only defined for integer values of n, corresponding to big dots on the two continuous curves. The chemical potential μ_n is monotonic function of the distance between the n^{th} dot and the horizontal axis. A preference for a high number of layers is therefore obtained in that example.

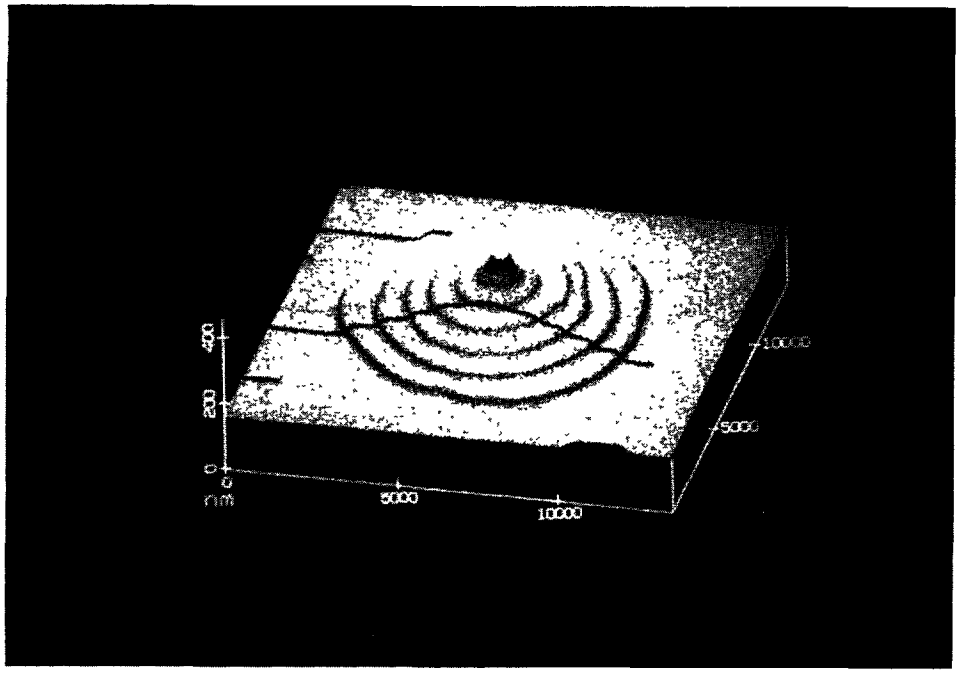

Fig. 4. — Ziggourat-like structure obtained after annealing at 170 °C for one day a thin film of a symmetric (Polystyrene-polymethylmetacrylate) diblock copolymer of mass 57 000, with a thickness initially uniform, as observed by Atomic Force Microscopy. Each step between two circular terraces has the same height $L = 290 \pm 10$ Å, identical to the lamellar periodicity.

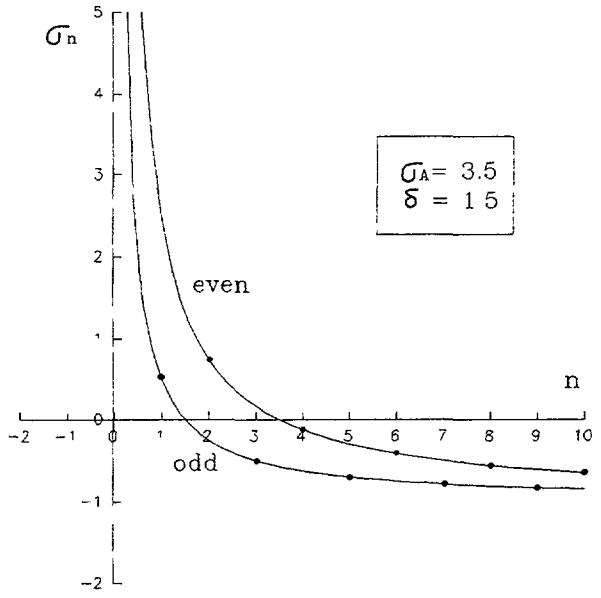

Fig. 5. — σ_n *versus* n for $\sigma_A = 5.5$ and $\delta = 2$. n-layers corresponding to big dots above the n-axis are spreading completely on the solid substrate. Their chemical potential is not defined. Dots below the n-axis correspond to metastable state, with one preferential state n^* for each parity. In this example, the lowest chemical potential is obtained for n^* even, which is only metastable however.

3.2 $\sigma_A - \delta^{up} \geqslant 0$. — In this section we consider situations where $\sigma_A - \delta$ is high enough so that $\sigma_n > 0$ for at least one value of n. In other words, $\sigma_A > 2$ if n is even and $\sigma_A > 1 + \delta$ if n is odd. On increasing n, σ_n becomes negative at $n = n^*$ and tends to $-\gamma_{AB}$ as $n \to \infty$. Thus for $n < n^*$, the condition for spreading is satisfied. For $n \geqslant n^*$, metastable states are obtained with the state $n = n^*$ having the lowest energy. Note that even this state is only metastable as the energy of the film decreases without bound when it spreads on the solid surface. This situation is illustrated in figure 5.

3.3 INTERMEDIATE CASE.

$$\delta < \sigma_A < 1 + \delta \quad (n \text{ odd}) \tag{17}$$

$$0 < \sigma_A < 2 \quad (n \text{ even}) \tag{18}$$

3.3.1. — In the narrow range of values of σ_A defined by the above two conditions, σ_n is again a decreasing function of n, but it is always negative. Therefore, a given film cannot spread. All states are metastable and the chemical potential increases with n. Hence there is one absolutely stable state which is either the monolayer or the bilayer. It is a bilayer if $\mu_2 < \mu_1$, i.e., if

$$\sigma_A < 2\,\delta\,. \tag{19}$$

Figure 6 shows the variation of σ_n with n for such a situation. A necessary condition for satisfying the above three conditions is that $0 < \delta < 2$.

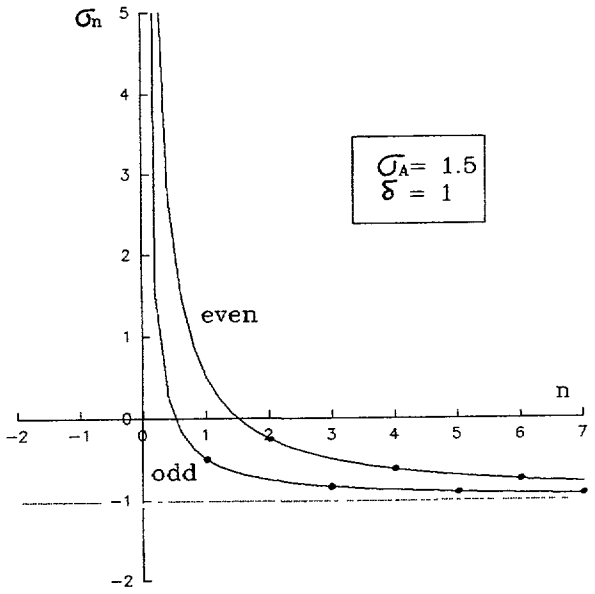

Fig. 6. — σ_n *versus* n for $\sigma_A = 1.5$ and $\delta = 1$. There is no spreading n-layer since no dot is found above the n-axis. The big dot which is the closest from the axis is at $n = 2$. The bilayer is therefore stable.

3.3.2. — Let us now consider a situation where (17) is satisfied but not (18). There are two possibilities ; either $\sigma_A < 0$ or $\sigma_A > 2$.

i) $\sigma_A < 0$.

A necessary condition is that $\delta < 0$. Then the even n states fall into case a and are all metastable with the chemical potential decreasing with increasing n. The chemical potential of any odd state is smaller than that of any of the even parity states. If the system is initially in an even state, it can be expected to switch parity and finally reach the absolutely stable monolayer. This situation is illustrated in figure 7.

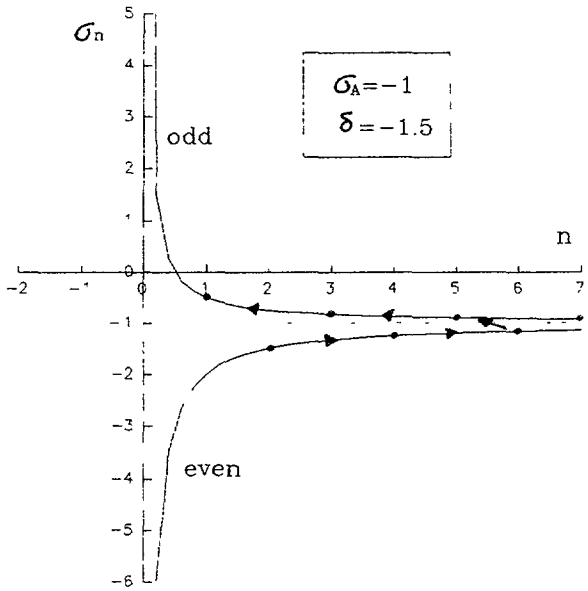

Fig. 7. — σ_n *versus* n for $\sigma_A = -1$ and $\delta = -1.5$. The monolayer is absolutely stable. A possible evolution of an initial bilayer is shown by the arrows.

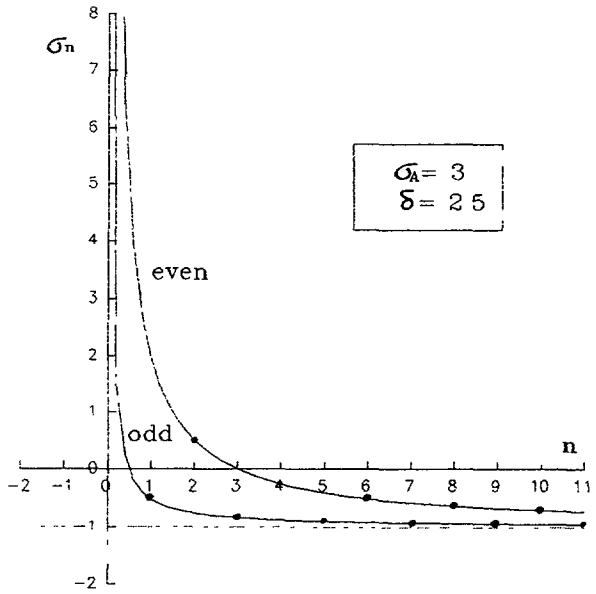

Fig. 8. — σ_n *versus* n for $\sigma_A = 3$ and $\delta = 2.5$. The monolayer is only metastable, since the dot for the bilayer is above the n-axis, meaning that the bilayer is spreading.

ii) $\sigma_A > 2$.

A necessary condition is that $\delta > 1$. In this case the bilayer and possibly some of the higher order even states are unstable and spread on the solid surface. The monolayer is metastable as switching to the bilayer leads to complete wetting, thus lowering the energy of the system. Such a case is illustrated in figure 8.

3.3.3. — We finally consider the case where (18) is satisfied but not (17). There are again two possibilities ; either $\sigma_A < \delta$ or $\sigma_A > 1 + \delta$.

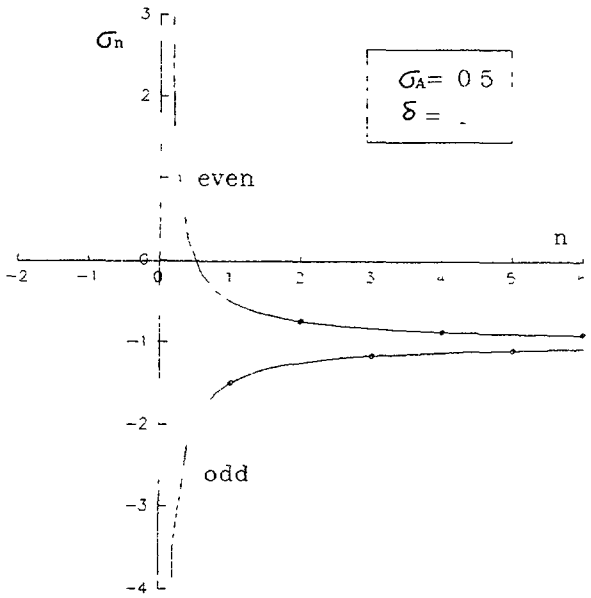

Fig. 9. — σ_n *versus* n for $\sigma_A = 0.5$ and $\delta = 1$. Odd states are piling up, while even states prefer lowest n. The bilayer is absolutely stable.

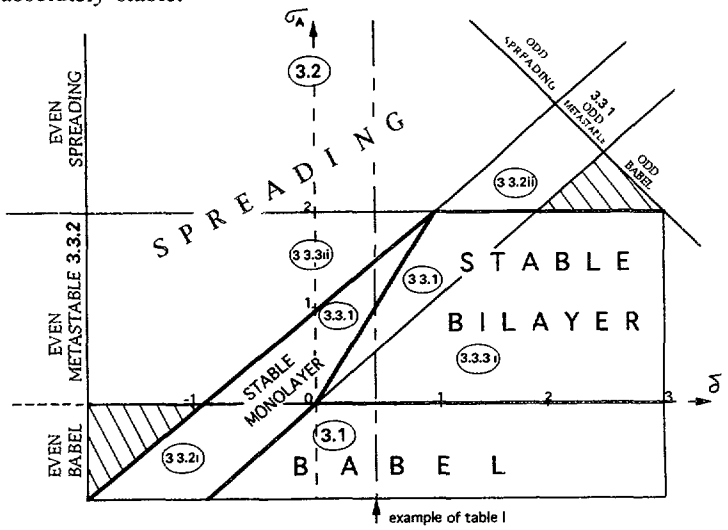

Fig. 10. — Diagramm of all possible regimes in the (δ, σ_A) space. Types enclosed in ellipses refer to the corresponding sections in the text. Heavy lines define four main regimes defined on the basis of the lowest energy state : spreading ; monolayer ; bilayer ; and Babel. Thin lines divide these principal areas in subregions with uniform behaviours. The pathologic situations mentioned in the text are found in dashed areas.

i) $\sigma_A < \delta$.

The necessary condition on δ is that $\delta > 0$. This situation is similar to the one of figure 7 (section 3.3.2 ; i)) with odd and even parities inverted. The bilayer is now absolutely stable as can be seen from figure 9.

ii) $\sigma_A > 1 + \delta$.

A necessary condition on δ is that $\delta < 1$. The odd parity states fall into case 3.2 and spread. The bilayer is now metastable. The case is very similar to the one illustrated in figure 8 for opposite parities.

All the discussion above has been summarized in the diagramm of figure 10 drawn in the (δ, σ_A) space. To illustrate how to use it in practice, let us consider an example with $\delta = 1/2$. Depending on σ_A, several behaviours can be encountered. They are graphically summarized below :

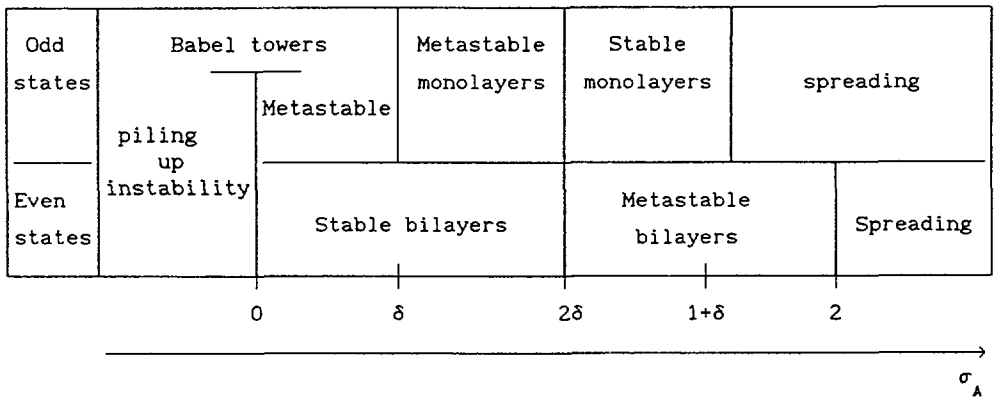

The two dashed area have been left apart in the discussion. They correspond to the strange situation where films belonging to one parity are spreading while those belonging to the other are piling up.

4. Grafted monolayer.

So far in this paper we have assumed that the polymer chains are free to move along the solid surface. However, in many practical situations it need not be so. Therefore, we now consider the case where the first copolymer monolayer is grafted onto the solid substrate. Then the solid surface behaves like a plane polymer melt surface. For connection with the previous sections, one assumes that the species B is grafted and that the species A is exposed to the air. One should also relax the earlier conventions embodied in (8) and (9) concerning A and B denominations. Further, the quantities γ_{SV}, γ_{LV}^{A}, γ_{LS}^{B} have to be replaced respectively by γ_{LV}^{A}, 0, γ_{AB}, 0 and $\Delta\gamma - \gamma_{AB}$.

- If we have A against the surface, the dimensionless spreading parameter is given by

$$\sigma_n = -(1/n)\,\delta^{up} - 1 .$$

If δ is positive even states are prefered. They are all stable with the same chemical potential. Consequently, rough surfaces can develop with time. On the other hand, if $\delta < 0$, odd states are prefered, with : i) stable monolayer and metastable multilayers if $-1 < \delta < 0$; ii) all states spreading if $\delta < -1$.

• If we have B against the surface, then

$$\sigma_n = -(1/n) - 1 \qquad n \text{ odd}$$
$$\sigma_n = -(1/n)(1+\delta) - 1 \qquad n \text{ even}.$$

A necessary condition for the surface to prefer B over A is that

$$|\sigma_n| \leqslant 1 .$$

This is possible for the even states if $(\mathrm{d}\sigma_n/\mathrm{d}n) < 0$, i.e., if $\delta < -1$. But this is precisely the spreading condition when A is against the surface. Hence no stable state can be obtained with B against the surface.

As an additional remark we underline that moving δ across 0 corresponds in principle to a roughening transition. Since γ_{AB}, γ^{B}_{LV} and γ^{A}_{LV} are temperature dependent, it should be possible to obtain a temperature controled roughening transition by the right choice of A and B. As an example, let us mention the polystyrene/polymethylmethacrylate copolymer as a reasonable candidate.

5. On a possible reversible temperature induced wetting-dewetting transition.

Consider a stable monolayer of thickness ℓ_0 lying on a solid substrate. On increasing the temperature above T_{OD}, the film melts into a homogeneous mixture of the two species A and B. As the A-B interface has disappeared, the spreading condition is now that for a simple liquid given by equation (1). It is possible that $S_M > 0$ for the homogeneous melt, although $S_1 < 0$ for the monolayer, as the former expression does not contain the $-\gamma_{AB}$ term. Hence we can induce a reversible wetting-dewetting transition by changing the temperature. The

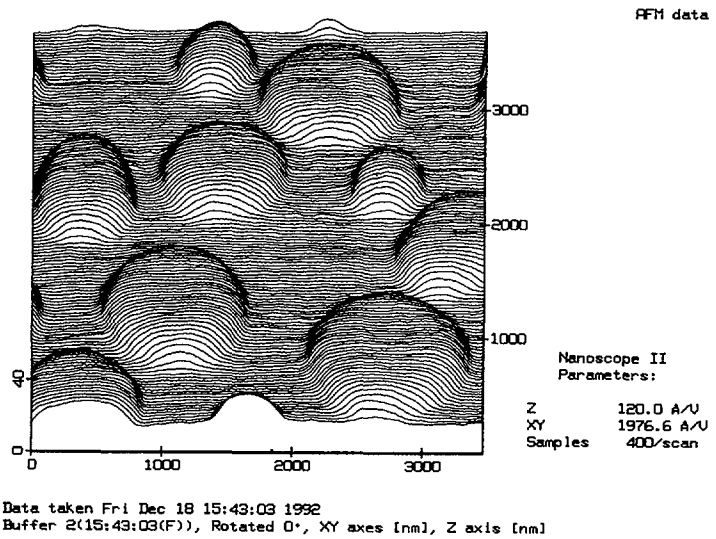

Fig. 11. — Disconnected islands of height $\ell_0(1) = 160 \pm 10$ Å visualized by atomic force microscopy. The copolymer is a symmetric PS-PMMA dibloc of molecular mass 57 000, and the substrate a silicon wafer. The initial film was solid and homogeneous in thickness. The present structure has been obtained by annealing it at $T < T_{OD}$ for 24 hours. Further annealing for one month was unable to modify the island population.

topology of the monolayer obtained on cooling an initially spread film of thickness ℓ at $T > T_{OD}$ can be expected to depend on ℓ. If $\ell \ll \ell_0/2$, ℓ_0 being the equilibrium monolayer thickness, the monolayer will consist of disconnected islands of thickness ℓ_0. Once formed, no kinetic evolution is possible except by diffusion of the islands as a whole. Such a structure is shown in figure 11. On the other hand, if $\ell_0/2 \ll \ell < \ell_0$, the monolayer would have a distribution of holes in it. A slow growth process driven by the line tension should lead to their ultimate disappearance. If $\ell \sim \ell_0/2$, the dewetting should result in the formation of a bicontinuous labyrinth of wet and dewet regions. The slow evolution process can then be expected to lead to several large disconnected domains.

To summarize, the essential conclusion of the present work is that the possible equilibrium states of a non-grafted copolymer film reduce to monolayers or bilayers. Every n-layer with $n > 2$ is therefore unstable (spreading) or metastable (piling up). The second important feature is that the ordered copolymer is more likely to be non-wetting compared to the homogeneous melt of the same composition. This leads to the possibility of a temperature controled wetting-dewetting transition, driven by the appearance or disappearance of the A-B interface. The third feature is the formation of characteristic Babel towers in the piling up instability. Their shape, however, cannot be understood within the static picture used in this study. The case of a grafted monolayer leads to the interesting possibility of the spontaneous roughening of the copolymer film deposited on it. A complete understanding of all the experimentally observed behaviours would now require to go into the dynamics of these systems.

References

[1] Bates F. S., Fredrickson G. H., *Annu. Rev. Phys. Chem.* **41** (1990) 525.
[2] de Gennes P. G., *Rev. Mod. Phys.* **57** (1985) 827.
[3] See e.g. Turner M. S., *Phys. Rev. Lett.* **69** (1992) 1788.